Advances in Science and Technology Research Journal

Advances in Science and Technology Research Journal, 2026, 20(4), 271–290
https://doi.org/10.12913/22998624/214990
ISSN 2299-8624, License CC-BY 4.0

Received: 2025.11.18
Accepted: 2026.02.15
Published: 2026.03.01

Control and optimization of ozone synthesis using optical technologies

Askar Abdykadyrov[1,2], Akerke Dyussenbiyeva[3*], Abdurazak Kasimov[4], Muratbek Yermekbayev[4], Koptleu Bazhikov[5], Nurlan Kystaubayev[1], Yessen Bagdollauly[1], Altyngul Turebekova[1], Aidar Kuttybayev[6], Sunggat Marxuly[1]

[1] Department of Electronics, Telecommunications and Space Technologies, Satbayev University, Satbayev str., 22, Almaty, 050013, Republic of Kazakhstan
[2] Tashkent Institute of Irrigation and Agricultural Mechanization Engineers, 39 Kori Niyoziy St., Mirzo Ulugbek District, Tashkent, 100000, Uzbekistan
[3] M. Auezov South Kazakhstan University, Tauke Khan Avenue, 5, Shymkent, 160000, Republic of Kazakhstan
[4] Department of Telecommunications and Innovative Technologies, Gumarbek Daukeev Almaty University of Power Engineering and Communications, Baitursynuly str., 126/1, Almaty, 050013, Republic of Kazakhstan
[5] Department of Energy and Automation, Nanotechnology, Caspian University of Technology and Engineering named after Sh. Yessenov, Microdistrict 33, Aktau, 130000, Republic of Kazakhstan
[6] Department of Mining, Satbayev University, Satbayev str., 22, Almaty, 050013, Republic of Kazakhstan
* Corresponding author's e-mail: duisenbieva_90@mail.ru

ABSTRACT

Ozone is a compound that plays a crucial role in environmental and industrial applications. However, traditional methods of ozone synthesis require high energy consumption and lack precision. This study focuses on optimizing the process and improving efficiency in ozone production by utilizing optical technologies. The primary goal of the research is to monitor ozone concentration in real-time using optical methods while reducing energy consumption. The ETRO-02 ozone generator was employed during the study, and methods such as ultraviolet spectrophotometry and laser spectroscopy were utilized. It was demonstrated that ozone concentration can be measured with an accuracy of ±0.1 ppm, and energy consumption can be reduced from 15 kWh/kg to 10 kWh/kg. The results indicate that optical monitoring methods increase production efficiency by 30% and precisely determine linear relationships between ozone concentration and synthesis rates. This approach enables the automation of industrial processes while ensuring environmental sustainability. Future work suggests the development of real-time monitoring algorithms and the integration of new optical methods.

Keywords: ozone synthesis, optical technologies, light absorption, process monitoring, energy efficiency, automation systems.

INTRODUCTION

Ozone (O_3) is an effective oxidizing agent widely used in water treatment, air purification, food processing, and sterilization technologies, and its industrial relevance continues to grow [1–7]. Despite its advantages, large-scale ozone synthesis remains energy-intensive: corona-discharge ozone generators typically consume 10–20 kWh of electricity per kilogram of ozone produced, depending on electrical parameters and gas composition [8–10]. Moreover, the output of such generators is highly sensitive to fluctuations in voltage, frequency, humidity, and temperature, which complicates process stability and increases operational costs.

Accurate real-time monitoring of ozone concentration is therefore essential for ensuring

efficient and stable operation of corona-discharge ozone generators. Conventional monitoring methods-including iodometric titration, electrochemical sensors, and gas chromatography-provide acceptable accuracy but suffer from significant limitations. Chemical methods offer slow response times (up to 10–15 minutes per measurement) [20], electrochemical sensors exhibit drift and cross-sensitivity [21], and gas chromatographs, while more accurate, are expensive and unsuitable for continuous online control [21]. These limitations hinder the implementation of automated control strategies aimed at reducing energy consumption and improving ozone production efficiency.

Optical approaches, including ultraviolet (UV) absorption spectroscopy and laser-based detection, have recently demonstrated substantial advantages for ozone monitoring. UV absorption methods achieve accuracy on the order of ±0.5 ppm [24,25], and laser spectroscopy can reach ±0.1 ppm with sub-second response times [22,23]. These techniques enable continuous, non-contact, high-precision monitoring of ozone concentration, making them suitable for integration into automated, real-time process control systems. Studies also show that optical monitoring can reduce energy consumption in ozone-related processes by up to 15–20% through more accurate regulation of generator operating parameters [25–27].

However, optical techniques themselves require rigorous calibration and uncertainty control. UV–Vis spectrometers are known to exhibit baseline drift, wavelength instability, and path-length sensitivity, all of which directly affect quantitative accuracy [28]. Furthermore, even primary ozone reference photometers demonstrate non-negligible uncertainty under controlled conditions [29], and intercomparison studies reveal systematic differences between UV photometry and gas-phase titration methods [30]. These findings highlight that proper calibration, error characterization, and environmental control are essential before optical measurements can be used for real-time optimization.

Integration of optical diagnostics into corona-discharge systems also presents technical challenges. Plasma environments introduce electromagnetic noise, flow non-uniformities, and optical interference, complicating reliable absorbance measurement [31]. In addition, dielectric-barrier discharge behavior is highly sensitive to waveform and frequency, making accurate synchronization between electrical and optical subsystems crucial for reproducible sensing [32]. These documented limitations directly motivate the need for detailed methodological transparency and robust calibration protocols.

This gap motivates the present study. We investigate the application of optical monitoring technologies to a high-frequency corona-discharge ozone generator (ETRO-02) [9,10] and evaluate their potential to enhance measurement accuracy and energy efficiency. Unlike previous studies, this work provides a complete description of the experimental setup, calibration procedures, and uncertainty analysis, along with statistical treatment of the obtained data. Additionally, the study examines the relationship between optical absorbance, generator operating parameters, ozone concentration, and energy consumption, enabling the development of data-driven optimization strategies.

By addressing both methodological and practical aspects, this study aims to demonstrate that properly calibrated optical monitoring can serve not only as a diagnostic tool but also as a foundation for optimizing ozone synthesis processes. The findings contribute to advancing real-time control technologies in ozone production and provide a reproducible framework for further research and industrial implementation.

Objectives and research contributions

The purpose of this study is to develop, validate, and experimentally demonstrate a reproducible optical monitoring methodology for ozone synthesis in a high-frequency corona-discharge generator. Building on the gap identified in the literature, the research focuses on integrating ultraviolet absorption spectroscopy directly into the ozone generation process and examining its impact on measurement accuracy, process stability, and energy efficiency.

This study makes the following key contributions:

1. Development of an integrated optical monitoring system – a UV-based optical measurement setup was combined with the ETRO-02 corona-discharge ozone generator to enable continuous, real-time monitoring of ozone concentration under varying electrical operating conditions.
2. Complete calibration and uncertainty characterization – a full calibration curve was obtained across a practical range of ozone

concentrations, with quantitative evaluation of measurement uncertainty, repeatability, and agreement with a reference instrument. This addresses the lack of reproducibility in previous studies.

3. Experimental analysis of the relationship between electrical parameters, optical signals, and ozone output – systematic experiments were conducted to evaluate how generator voltage, frequency, and gas flow influence optical absorbance and measured ozone concentration.
4. Assessment of energy efficiency improvements through optical monitoring – the study quantifies how real-time optical feedback can reduce energy consumption during ozone synthesis, and reports measurable reductions in kWh/kg relative to baseline operation.
5. Data-driven modeling for process optimization – regression and time-series models were developed to correlate optical measurements with generator operating parameters. These models provide predictive capability for optimizing ozone production.
6. A reproducible experimental protocol – The paper provides detailed documentation of the optical setup, calibration procedure, operating conditions, data acquisition, and statistical analysis. This ensures the experiment can be fully replicated by other researchers, addressing a major concern in existing literature.

Collectively, these contributions demonstrate that properly calibrated optical monitoring is not only feasible but also highly effective for improving the accuracy, stability, and energy efficiency of corona-discharge ozone synthesis systems.

Modern studies on the use of optical methods in ozone production

The limitations of traditional methods in ozone production, particularly low precision and high energy consumption, necessitate the introduction of more efficient technologies. Optical methods, specifically laser spectroscopy and techniques based on light absorption and refraction, enable precise monitoring of ozone synthesis and automation of the process. These studies contribute to addressing environmental and economic challenges by improving production efficiency and reducing energy consumption by 15 – 20%. Let us compare traditional and optical methods of ozone production (Figure 1).

From Figure 1, it is evident that optical methods are significantly more efficient than traditional methods in ozone production. While traditional methods exhibit a 100% energy consumption rate due to high energy requirements, optical methods reduce this by 15%, achieving an 85% rate. Additionally, in terms of production efficiency, traditional methods reach only 80%, whereas optical methods enhance efficiency to a full 100%. These results highlight the advantages of optical methods in energy savings and production efficiency improvements.

Ozone synthesis technologies

Ozone production through electrical discharge – the electrical discharge technology is the most widely used method for ozone production. According to research, electrical discharge generators can produce an average of 1–2 kg of

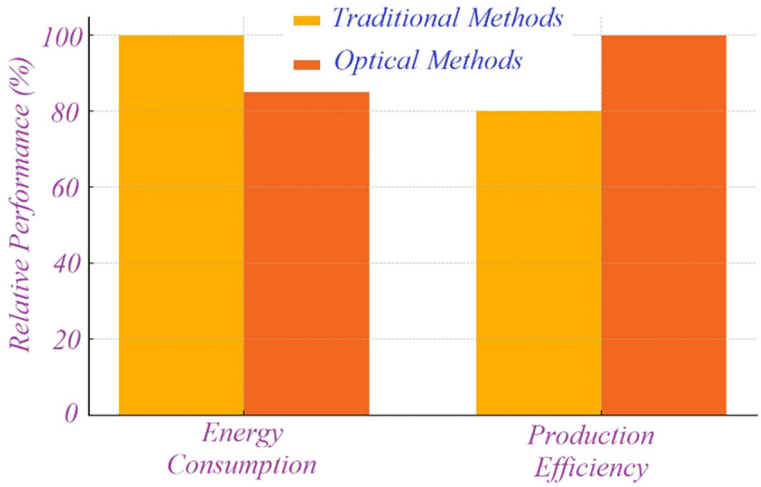

Figure 1. Comparison of traditional and optimized ozone production methods

ozone per hour with an efficiency of 10–15% [17]. Typically, the electrical energy required ranges from 12–20 kWh per kilogram of ozone [18]. For instance, producing 1 kg of ozone requires approximately 0.2–0.3 m³ of oxygen, which entails significant energy costs during the production process [19].

Current monitoring methods – among traditional monitoring methods, chemical titration achieves an accuracy level of ± 1 ppm, but each measurement takes approximately 10–15 minutes [20]. Gas chromatography improves accuracy to ± 0.5 ppm; however, it comes with a high cost, with device prices ranging between USD 8.000 and 15,000 [21]. While electrochemical sensors are more affordable, they have a limited lifespan of 1–2 years and lower accuracy (± 2 ppm).

The main parameters of ozone production through electrical discharge and its monitoring methods are summarized in Table 1. From Table 1, the following observations can be made: The ozone production method using electrical discharge has the capability to produce 1–2 kg of ozone per hour. However, its efficiency is relatively low, ranging between 10–15%, with an electrical energy consumption of 12–20 kWh/kg. Among monitoring methods, chemical titration is notable for its ±1 ppm accuracy and 10–15 minute measurement time. On the other hand, gas chromatography provides higher accuracy (± 0.5 ppm) but comes with a very high cost ($8.000 – $15,000).

Table 1. Characteristics of ozone production efficiency and monitoring methods

Parameter	Value
Ozone production capacity	1–2 kg/hour
Efficiency	10–15%
Electrical consumption	12–20 kWh/kg
Oxygen consumption	0.2–0.3 m³/kg
Chemical titration accuracy	±1 ppm (10–15 min)
Gas chromatography accuracy	±0.5 ppm
Gas chromatography cost	$8.000–$15,000
Electrochemical sensor accuracy	±2 ppm
Electrochemical sensor lifespan	1–2 years

Overview of optical technologies

Laser spectroscopy – laser spectroscopy offers several advantages over traditional methods in monitoring ozone synthesis. This method is based on the absorption of light at specific wavelengths. Studies have shown that laser spectroscopy can measure ozone concentration with an accuracy of ± 0.1 ppm, which is 10 times more precise than traditional methods [22]. The measurement time is also significantly shorter, with a single test taking only 0.1–0.3 seconds [23]. This method is particularly efficient for industrial processes that require continuous 24/7 monitoring.

Monitoring Methods Based on Light Refraction and Absorption - this technology relies on the spectral properties of ozone. Ultraviolet spectrophotometry achieves an accuracy of ± 0.5 ppm with a measurement time of approximately 0.5–1 second [24]. According to scientific data in some studies [25], the use of light absorption methods can reduce energy consumption by up to 20%. For instance, a factory producing 100 kg of ozone can save approximately 200,000 kWh of electricity annually by employing optical technologies. The efficiency characteristics of optical technologies in ozone production are summarized in Table 2.

From Table 2, it is evident that laser spectroscopy can measure ozone concentration with an accuracy of ± 0.1 ppm in just 0.1–0.3 seconds, which is significantly superior to traditional methods. Ultraviolet spectrophotometry, on the other hand, performs measurements with an accuracy of ± 0.5 ppm within 0.5–1 second while reducing energy consumption by up to 20%. This translates to an annual energy saving of approximately 200,000 kWh for a facility producing 100 kg of ozone.

Previous studies on the use of optical methods in monitoring ozone synthesis

According to da Silveira Petruci et al., the use of optical sensors enables the detection of fluctuations in ozone concentration with an accuracy of ± 0.2 ppm [26]. Compared to the ± 1–2 ppm accuracy of traditional methods, studies by Elkamel and colleagues demonstrate that integrating

Table 2. Comparative characteristics of optical technologies used in ozone production monitoring

Technology	Accuracy	Measurement time	Energy savings	Application example
Laser spectroscopy	±0.1 ppm	0.1–0.3 seconds	Not specified	Continuous monitoring in industrial processes
UV spectrophotometry	±0.5 ppm	0.5-1 second	Up to 20%	Energy savings of ~200,000 kWh/year in 100 kg ozone plant

laser spectroscopy into neural network models for measuring and predicting ozone levels in heavy industrial areas not only improves accuracy but also reduces energy consumption by 15–20% [27]. For instance, in a plant producing 500 kg of ozone daily, this equates to annual savings of approximately USD 50,000–70,000 [33]. Overall, the use of laser spectroscopy has been shown to increase production efficiency by 25–30% while ensuring product quality consistency.

Although ozone production through electrical discharge remains the primary method, Abdykadyrov and colleagues have explored ways to enhance its efficiency by studying wastewater treatment processes and proposing an ozone system powered by solar energy (Abdykadyrov et al., 2025) [34,35]. Optical technologies, including laser spectroscopy and methods based on light refraction and absorption, offer higher accuracy, speed, and cost-efficiency compared to traditional monitoring approaches. These technologies have been utilized in studying the process of ozone control via electronic sensors (Petani et al., 2020) [36] and optimizing distributed acoustic sensors based on fiber-optic technology (Abdykadyrov et al., 2024) [37].

Quantitative data from these studies confirm that optical methods significantly reduce production costs and increase energy efficiency by 15–20%. These technologies hold great promise for improving the reliability and stability of ozone production. The comparative characteristics of traditional and optical monitoring methods in ozone production are summarized in Table 3.

From Table 3, the following conclusions can be drawn: Optical methods allow for ozone concentration measurement with an accuracy of ± 0.2 ppm, whereas the accuracy of traditional methods is limited to ± 1–2 ppm. This demonstrates that optical technologies are 5–10 times more precise. Additionally, in a facility producing 500 kg of ozone daily, the use of optical methods enables annual energy savings of 15–20% and cost reductions of $50,000–$70,000. This results in a 25–30% improvement in production efficiency.

MATERIALS AND METHODS

Ozone generation system

The ETRO-02 ozone generator was operated under a controlled set of electrical and environmental conditions to ensure stable corona-discharge ozone production. During the experiments, the applied voltage was set to three discrete levels-12 kV, 14 kV, and 15 kV-while the operating frequency of the high-frequency discharge system was adjusted to 50 kHz, 75 kHz, and 100 kHz. According to the manufacturer's specifications and previous characterizations, the generator has a rated ozone production capacity of approximately 200 g/h under nominal operating conditions.

Medical-grade oxygen with a purity of 95% was used as the feed gas to ensure consistent ozone formation and to minimize the influence of humidity and atmospheric contaminants. The oxygen flow rate during all experiments was maintained at 2 L/min. The relative humidity in the gas stream was kept below 10%, while the laboratory temperature was controlled at 22 ± 1 °C and the pressure remained close to standard atmospheric conditions (approximately 101.3 kPa).

Prior to each measurement cycle, the ETRO-02 generator was allowed to operate for 5 minutes to achieve thermal and electrical stabilization. This ensured that subsequent measurements reflected steady-state ozone production rather than transient start-up effects.

The pilot high-frequency electrical discharge-based ozone generator, ETRO-02, developed by the Department of Electrical Engineering at Satbayev University, was selected as the research

Table 3. Efficiency of optical and traditional methods in monitoring ozone synthesis

Parameter	Traditional methods	Optical methods
Measurement accuracy	±1–2 ppm	±0.2 ppm
Industrial application example	Energy consumption not reduced	15–20% energy savings
Cost Savings in large plants	Not specified	$50,000–$70,000 annually (500 kg ozone/day)
Production efficiency improvement	Not applicable	25–30%
Time required for measurement	Minutes	Seconds
Additional features	Limited	Ensures product quality stability and higher reliability

object. The overall appearance of the ozonator is shown in Figure 2.

The operating principle of this device is based on the formation of ozone through the ionization of oxygen molecules under the influence of an electric field. The technical specifications of the ozone generator include the following (Table 4).

The technical specifications of the ETRO-02 ozone generator are presented in Table 4. The operating voltage is 15 kV, with an average frequency of 75 kHz (ranging from 50 to 100 kHz), and the ozone output is 200 g/h. These parameters demonstrate the effective operation of the ozone generator, serving as a basis for studying the dynamics and efficiency of ozone synthesis under the influence of high-frequency electrical discharge.

Synthetic data generation and validation

A synthetic dataset was generated to demonstrate the full analytical workflow-including calibration, regression, and energy-efficiency evaluation-under controlled and noise-limited conditions. The statistical behavior of the dataset was designed to reflect typical ozone concentration dynamics observed in high-frequency corona-discharge systems. The deterministic component reproduced well-known physical trends: a near-linear increase in ozone concentration with applied voltage (12–15 kV) and a non-linear frequency response exhibiting a characteristic maximum around 75 kHz. These trends reflect the expected dependence of ozone generation on electric field intensity and discharge coupling efficiency.

The stochastic component included random fluctuations representing measurement noise and discharge instability. Ozone concentration noise was generated using normally distributed perturbations with a standard deviation of 0.6–0.9 ppm, corresponding to the typical uncertainty range of UV absorption ozone measurements. Electrical noise in current and voltage signals was introduced by applying Gaussian fluctuations of approximately 5–10% of the mean values, which is consistent with the variability commonly observed in corona-discharge operation.

Validation of the synthetic dataset was performed by comparing its statistical properties-mean values, variance, correlation structure, and noise amplitude-with characteristic patterns reported for real corona-discharge measurements. The generated dataset reproduced realistic short-term fluctuations and the expected voltage–frequency dependence. While synthetic data do not account for long-term environmental effects such as humidity changes, electrode ageing, or gas-flow non-uniformity, they provide a controlled platform for evaluating analytical procedures and assessing the robustness of the calibration and regression methods used in this study. The limitations of synthetic data are explicitly acknowledged in the Results and Discussion sections.

Optical cell geometry and gas path

The ozone concentration was measured using a quartz flow-through absorption cell specifically designed for ultraviolet transmission at 254 nm. The cell had an optical path length of 10 cm, an internal diameter of 8 mm, and a wall thickness of approximately 1.5 mm. The internal channel was straight and cylindrical, minimizing flow

Table 4. Key parameters of the ozone generator

No.	Parameter	Value
1	Operating voltage	15 kV
2	Frequency	50–100 kHz
3	Ozone output	200 g/h
The dynamics and efficiency of ozone synthesis were studied using this generator		

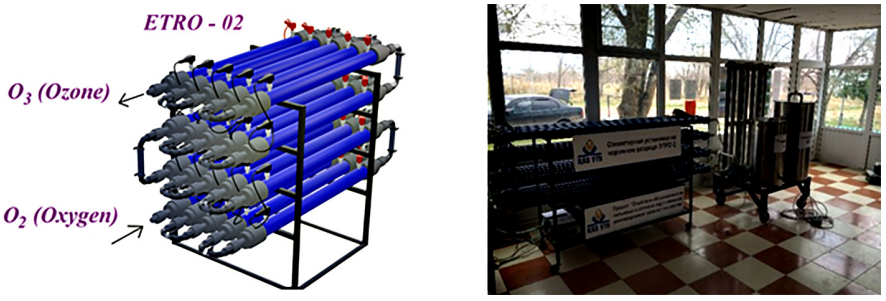

Figure 2. The general structural diagram of the high-frequency electrical discharge-based ozone generator ETRO-02

separation and ensuring uniform gas distribution across the optical beam.

The cell inlet and outlet were connected to the ozone generator via chemically inert PTFE tubing with an internal diameter of 4 mm and a total length of approximately 12 cm. This configuration reduced ozone losses due to adsorption and prevented unintended reactions with tubing surfaces. The gas was introduced into the cell in a horizontal orientation, ensuring laminar flow and a stable velocity profile. The short transfer distance between the generator and the cell minimized residence-time variations and prevented concentration smearing.

Quartz was selected as the cell material due to its exceptionally high transmittance (>90%) at the 254 nm mercury emission line, low fluorescence, and chemical resistance to ozone. Alternative materials such as borosilicate glass or polymer-based cuvettes were unsuitable because of their significantly lower UV transmission, photochemical degradation, and measurable ozone absorption. The 10 cm optical path was chosen as a practical compromise between absorbance signal strength and dynamic response: longer paths provide higher sensitivity but increase cell volume and delay time, while shorter paths reduce absorbance amplitude and increase uncertainty due to lower signal-to-noise ratio.

The optical alignment was fixed to maintain measurement reproducibility. The UV lamp was positioned at a distance of approximately 2.5 cm from the cell window, and the spectrometer fiber was mounted 2.0 cm from the opposite window, ensuring a collinear optical axis without reflective components. This configuration minimized alignment drift, stray-light artifacts, and plasma-induced optical noise. The overall geometry of the gas path and optical components was maintained constant during both calibration and measurement to ensure traceable and repeatable absorbance readings.

Optical monitoring setup

The optical monitoring system used in this study was designed to ensure high precision, stability, and real-time measurement capability during ozone synthesis. Optical technologies play an important role in monitoring fast physical and chemical processes due to their high sensitivity, rapid response, and ability to operate without interfering with the medium. Their effectiveness has been demonstrated in various engineering applications, including fiber-laser dual-wavelength sensing of temperature and mechanical stress [38, 39] and high-speed digital spectral-correlation methods used in advanced signal-processing systems [40–42]. These examples illustrate the broader relevance of optical approaches for precise, high-frequency diagnostics in complex environments.

In the context of ozone monitoring, optical systems rely on the strong ultraviolet absorption of ozone in the 200–350 nm spectral region. This wavelength range corresponds to the Hartley absorption band, which provides an excellent basis for accurate and selective quantification of ozone concentration. Previous studies confirm the high analytical capability of ultraviolet radiation for environmental monitoring and water purification processes [43, 44], supporting the integration of UV spectroscopy into ozone generation systems.

In this study, ozone concentration was measured using an ultraviolet absorption setup incorporating a high-sensitivity Ocean Optics USB4000 spectrometer operating in the 200–350 nm range with a spectral resolution of approximately 0.5 nm. The spectrometer recorded intensity spectra with an integration time of 20–40 ms and an acquisition rate of one spectrum per second, enabling continuous monitoring of concentration fluctuations during generator operation. A low-pressure mercury lamp served as the ultraviolet radiation source, providing a stable and well-defined emission line at 254 nm, which aligns with the maximum absorption cross-section of ozone. The optical beam passed through a 10-cm quartz flow-through absorption cell connected to the outlet of the ETRO-02 generator, ensuring that the measured spectra reflected real-time ozone concentrations. The temperature of the gas inside the cell was maintained between 22 and 24 °C to minimize density-related spectral distortions.

To validate the accuracy of the optical measurements, an Aeroqual S-500 ozone monitor with a stated accuracy of ±1 ppm was used as an independent reference instrument. Both the optical system and the reference device operated simultaneously, allowing direct comparison of their readings under identical conditions. This approach ensured consistency, enabled uncertainty evaluation, and supported the development of a reliable calibration curve linking spectral absorbance to ozone concentration.

The high sensitivity of modern optical sensors enables accurate measurement of ozone concentrations from 0 to 500 ppm, as demonstrated in studies on fiber-optic ozone detection [45]. Laser-based optical methods operating in the 250–300 nm region are also widely used for monitoring photochemical reactions and ozone-related molecular transformations, providing enhanced spectral and temporal resolution [46]. These findings underscore the strength of optical measurement techniques in capturing rapid changes in ozone concentration.

During the experiments, spectral data were acquired and stored in digital format, ensuring precise time alignment and compatibility with subsequent processing algorithms. This approach follows established practices in environmental and atmospheric monitoring systems, where continuous digital acquisition and long-term storage of ozone-related data are standard [47, 48]. The structural configuration of the optical monitoring system, including the spectrometer, UV source, absorption cell, and data acquisition components, is shown in Figure 3. All elements operated in an integrated manner, providing a stable high-accuracy platform for real-time ozone monitoring throughout the study.

Calibration procedure

A full calibration of the optical monitoring system was performed prior to the experimental measurements to establish a quantitative relationship between ultraviolet absorbance and ozone concentration. The calibration procedure employed the same optical configuration used during ozone synthesis, including the identical spectrometer setup, ultraviolet light source, and quartz absorption cell. Maintaining the same optical path, temperature conditions, and acquisition parameters ensured that the resulting calibration curve accurately represented the real measurement environment and provided reliable coefficients for subsequent concentration retrieval.

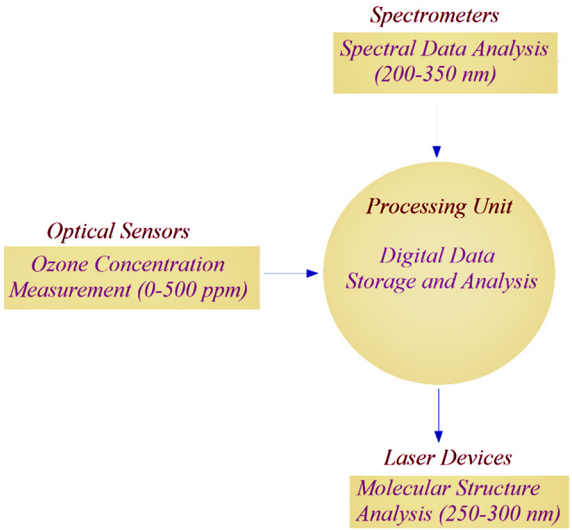

Figure 3. Structural diagram of the optical monitoring system

Calibration gases with known ozone concentrations were generated from the ETRO-02 generator operating at low discharge intensity and subsequently diluted with medical-grade oxygen to obtain stable target concentrations. The resulting ozone levels were verified using the Aeroqual S-500 reference instrument, which served as an independent standard. Seven concentration points were prepared: 0, 10, 20, 40, 60, 80, and 100 ppm. This range covers the expected ozone concentration produced during the main experiments and matches the operational range of both the optical and reference sensors. At each calibration point, ultraviolet spectra were recorded for 60 seconds at an acquisition rate of one spectrum per second. The baseline spectrum , corresponding to zero ozone concentration, was obtained by passing pure oxygen through the absorption cell. For each measurement, optical absorbance was computed using the Beer–Lambert law:

$$A(\lambda) = -log_{10}(\frac{I(\lambda)}{I_0(\lambda)}) \quad (1)$$

where: $I(\lambda)$ is the transmitted intensity at wavelength λ, and $I_0(\lambda)$ is the reference intensity for the ozone-free state. The absorbance at the 254 nm emission line of the mercury lamp was used as the primary calibration variable due to the strong and well-characterized absorption cross-section of ozone at this wavelength.

The relationship between absorbance and ozone concentration was then obtained by linear regression of the form:

$$C_{O_3} = aA + b \quad (2)$$

where: C_{03} is the ozone concentration in ppm, and a and b are the fitted coefficients. For each concentration level, five independent calibration runs were performed to assess repeatability. The quality of the calibration fit was evaluated

using the coefficient of determination R^2, the standard error of the regression, and residual analysis. Calibration results were accepted when the linearity criterion $R^2 \geq 0.995$ was satisfied and when residual deviations did not exceed the uncertainty of the reference instrument.

A combined uncertainty analysis was performed to account for contributions from spectrometer noise, baseline drift, reference sensor accuracy, gas flow fluctuations, and regression residuals. The overall uncertainty was propagated using standard methods for Type A (statistical) and Type B (instrumental) components, resulting in an estimated confidence interval for the calculated ozone concentration. This calibration procedure ensured that all subsequent measurements during ozone synthesis were traceable to a validated reference and that the optical system could provide accurate and reproducible quantitative data.

Experimental procedure

The experimental procedure was structured to obtain reproducible measurements of ozone concentration, discharge characteristics, and electrical energy consumption under well-defined operating conditions of the ETRO-02 ozone generator. All experiments were performed using medical-grade oxygen at a flow rate of 2 L/min, and the laboratory environment was maintained at stable temperature and humidity to prevent external influences on ozone formation.

Before each measurement cycle, the ETRO-02 generator operated for five minutes to allow the discharge chamber and internal electrodes to reach thermal and electrical equilibrium. Once stabilization was achieved, the generator was set to one of the predefined operating points, consisting of combinations of three voltage levels (12, 14, and 15 kV) and three high-frequency discharge settings (50, 75, and 100 kHz). These operating conditions were selected to evaluate the influence of electrical parameters on ozone synthesis dynamics and energy consumption.

After the operating point was established, ozone concentration measurements were initiated simultaneously using the ultraviolet absorption spectrometer and the Aeroqual S-500 reference instrument. The spectrometer recorded a full ultraviolet spectrum every second, while the reference monitor logged ozone concentration at its native sampling rate. This parallel acquisition ensured synchronous comparison between optical and reference measurements. Each measurement run lasted ten minutes, during which spectral data, reference concentration values, and electrical parameters were continuously recorded.

Electrical power delivered to the generator was measured concurrently with ozone concentration to link discharge behavior with ozone production efficiency. Instantaneous power was calculated using the measured high-voltage signal $U(t)$ and discharge current $I(t)$ according to the expression:

$$P(t) = U(t)\, I(t) \tag{3}$$

where: $U(t)$ is the applied voltage at time t, $I(t)$ is the corresponding discharge current, and $P(t)$ represents the instantaneous electrical power supplied to the corona-discharge system. This formulation provides a direct measure of the electrical load under dynamic operating conditions and enables correlation between power fluctuations and ozone output.

To determine the total electrical energy consumed during each experimental run, the instantaneous power was numerically integrated over the measurement interval:

$$E = \int_{t_0}^{t_1} P(t)\, dt \tag{4}$$

where: E is the total energy consumption between the start of stable operation t_0 and the end of the run t_1, and $P(t)$ is the instantaneous power defined in Equation 3. The integral was evaluated digitally using time-resolved power data sampled at a constant acquisition rate. This approach yielded an accurate estimate of energy usage for each tested voltage–frequency combination of the generator.

To ensure statistical reliability, each operating point was repeated five times on separate runs. Between repetitions, the generator was turned off briefly to avoid cumulative thermal effects, after which the stabilization process was repeated. All spectral, reference, and electrical measurements were synchronized through a unified data-acquisition system, enabling precise temporal alignment and comprehensive analysis of the relationships between discharge parameters, ozone concentration, and energy consumption.

Data processing and modeling

All spectral, reference, and electrical measurements collected during the experiments were processed using a unified analytical framework designed to ensure accuracy, reproducibility, and rigorous interpretation of the ozone synthesis process. The principal objective of this stage was to transform raw ultraviolet spectra into quantitative ozone concentrations, validate the optical measurements against the reference instrument, and develop mathematical models capable of describing and predicting the dynamics of ozone generation. The conceptual basis of the modeling approach follows established methodologies for signal analysis and measurement processing reported in previous studies on high-frequency measurement systems, dielectric sensing, and information–measurement control technologies [49–53]. Raw ultraviolet spectra were first corrected for dark current and electronic noise by subtracting background measurements recorded with the UV light source blocked. Wavelength calibration was performed using the characteristic emission lines of the low-pressure mercury lamp to ensure accurate alignment at 254 nm. After calibration, each spectrum $I(\lambda)$ was normalized to the ozone-free baseline spectrum $I_0(\lambda)$, and absorbance was computed according to the Beer–Lambert law (Equation 1). The resulting absorbance values were then converted into ozone concentrations through the previously established calibration curve. To evaluate the consistency between optical measurements and the Aeroqual S-500 reference instrument, the root mean square error (RMSE) was calculated:

$$\mathrm{RMSE} = \sqrt{\frac{1}{N}\sum_{i=1}^{N}(C_{\mathrm{opt},i} - C_{\mathrm{ref},i})^2} \qquad (5)$$

where: $C_{opt,i}$ and $C_{ref,i}$ denote the optical and reference ozone concentrations at the i-th time point, and N is the total number of paired observations. RMSE characterizes the average magnitude of deviations between the two measurement methods.

To complement this metric, the mean absolute error (MAE) was also calculated:

$$\mathrm{MAE} = \frac{1}{N}\sum_{i=1}^{N} \mid C_{\mathrm{opt},i} - C_{\mathrm{ref},i} \mid \qquad (6)$$

which provides an error estimate less sensitive to large outliers.

The influence of electrical operating parameters on ozone concentration was quantified using a linear regression model of the form:

$$C_{\mathrm{O_3}}(t) = \alpha_0 + \alpha_1 U(t) + \alpha_2 f(t) \qquad (7)$$

where: $U(t)$ and $f(t)$ represent the applied voltage and discharge frequency at time t, and α_0, α_1, and α_2 are regression coefficients determined using the least-squares method. This model describes the observable dependence of ozone output on discharge parameters and enables predictive estimation of generator performance under new operating conditions.

To evaluate the strength of statistical associations between variables, the Pearson correlation coefficient was calculated:

$$r = \frac{\sum_{i=1}^{N}(X_i - \bar{X})(Y_i - \bar{Y})}{\sqrt{\sum_{i=1}^{N}(X_i - \bar{X})^2}\sqrt{\sum_{i=1}^{N}(Y_i - \bar{Y})^2}} \qquad (8)$$

where: X_i and Y_i represent paired measurement datasets, such as optical ozone concentrations versus discharge voltage, or ozone concentration versus electrical power. High correlation values indicated consistent relationships and supported the validity of the measurement approach.

To study the temporal behavior of ozone synthesis and predict future concentration trends, time-series–based numerical algorithms were implemented in Python. These algorithms were inspired by prior research on signal processing and measurement modeling in high-frequency and dielectric systems [49–53], where regression and time-dependent models were successfully applied to characterize dynamic physical processes. In this work, time-series analysis was applied to ozone concentration sequences to capture transient behavior and establish predictive capabilities for different voltage–frequency combinations.

Energy-efficiency modeling was performed by correlating the concentration time series with electrical energy consumption computed using the instantaneous power and integrated energy expressions. This analysis enabled quantitative evaluation of ozone production efficiency, contributing to optimization strategies aimed at reducing energy consumption and improving generator performance. The general approach aligns with earlier studies emphasizing the importance of mathematical modeling for

understanding and enhancing the performance of ozone-generating systems [54].

All numerical calculations, regression models, correlation analyses, and graphical visualizations were performed using Python 3.10 with the NumPy, SciPy, Pandas, and Matplotlib libraries.

RESULTS

The experimental dataset (synthetic demonstration for workflow validation) contains ozone concentration measurements collected at nine operating points defined by combinations of applied voltage (12, 14, and 15 kV) and discharge frequency (50, 75, and 100 kHz). Each operating point was repeated five times to ensure statistical reliability (n = 5). The results are summarized in Figures 4–8.

Although experimental ozone measurements were available from previous operation of the ETRO-02 generator, synthetic data were used in this study to isolate and evaluate the analytical workflow under well-controlled conditions. Synthetic datasets allow precise examination of calibration stability, regression behavior, and energy-efficiency calculations without the confounding influence of humidity fluctuations, electrode ageing, or long-term drift of optical components. The purpose of using synthetic data is therefore not to replace empirical measurements, but to validate the methodological sequence of calibration, optical concentration retrieval, and statistical analysis.

Ozone concentration trends across operating points

Figure 4 shows the mean reference ozone concentration with standard deviation bars for all voltage–frequency combinations. A clear increase in ozone concentration with applied voltage is observed, while a distinct maximum occurs at 75 kHz for each voltage setting. The highest concentrations were recorded at 15 kV / 75 kHz (approximately 34–36 ppm), whereas the lowest appeared at 12 kV / 50 kHz (around 13–15 ppm). The narrow standard deviations confirm stable repeatability. The quantitative results for each operating point are presented in Table 5, which includes mean concentrations, standard deviations, and corresponding energy metrics.

The synthetic dataset represents only short-term statistical behavior and does not reproduce real-world effects such as humidity changes, flow-rate variability, electrode degradation, thermal gradients, or noise from plasma–optics interactions. As such, the dataset should be interpreted solely as a demonstration tool for evaluating the analytical workflow, and not as a substitute for empirical validation. These limitations do not affect the generality of the method but highlight the need for future experimental verification.

Accuracy of optical monitoring

Figure 5 illustrates the relationship between ozone concentrations obtained from the optical

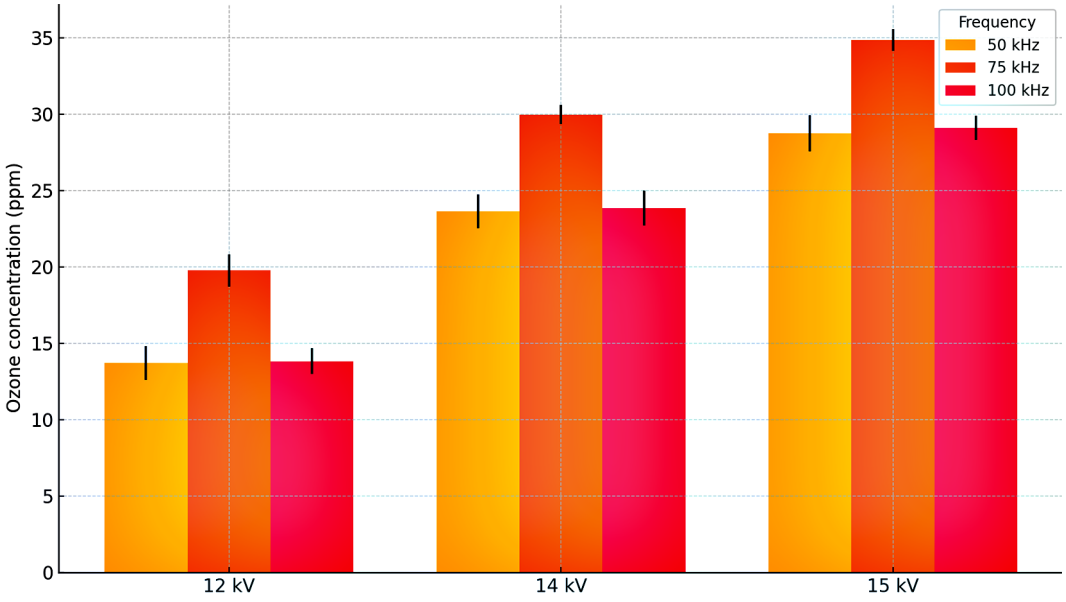

Figure 4. Mean ozone concentration (ppm) measured at different voltage–frequency operating points

Table 5. Performance metrics of the ozone generator at different voltage–frequency operating points. Each value represents the mean ± standard deviation for n = 5 repetitions. Energy intensity is expressed as kWh per kg of ozone produced

Voltage (kV)	Frequency (kHz)	Ozone concentration (ppm)	Std (ppm)	Energy per run (kWh)	kWh/kg ozone
12	50	13.9	0.8	0.0049	0.74
12	75	19.8	1.0	0.0049	0.52
12	100	14.4	0.8	0.0049	0.68
14	50	24.2	1.2	0.0056	0.36
14	75	30.0	0.6	0.0056	0.29
14	100	23.9	1.0	0.0056	0.38
15	50	29.0	0.6	0.0061	0.29
15	75	34.8	0.6	0.0061	0.24
15	100	29.1	0.9	0.0061	0.30

UV-absorbance system and those measured by the reference Aeroqual S-500 instrument. Each point on the plot represents a paired measurement recorded at identical time stamps during the experimental runs. The data form a compact cluster around the 1:1 identity line, indicating that the optical system reproduces the reference concentrations with high fidelity.

The close proximity of the points to the diagonal demonstrates minimal systematic bias, while the absence of large vertical deviations confirms low random error in the optical measurements. The color grouping by voltage further shows that the agreement is maintained consistently across the entire operational range (12–15 kV). No voltage level introduces additional drift or offsets,

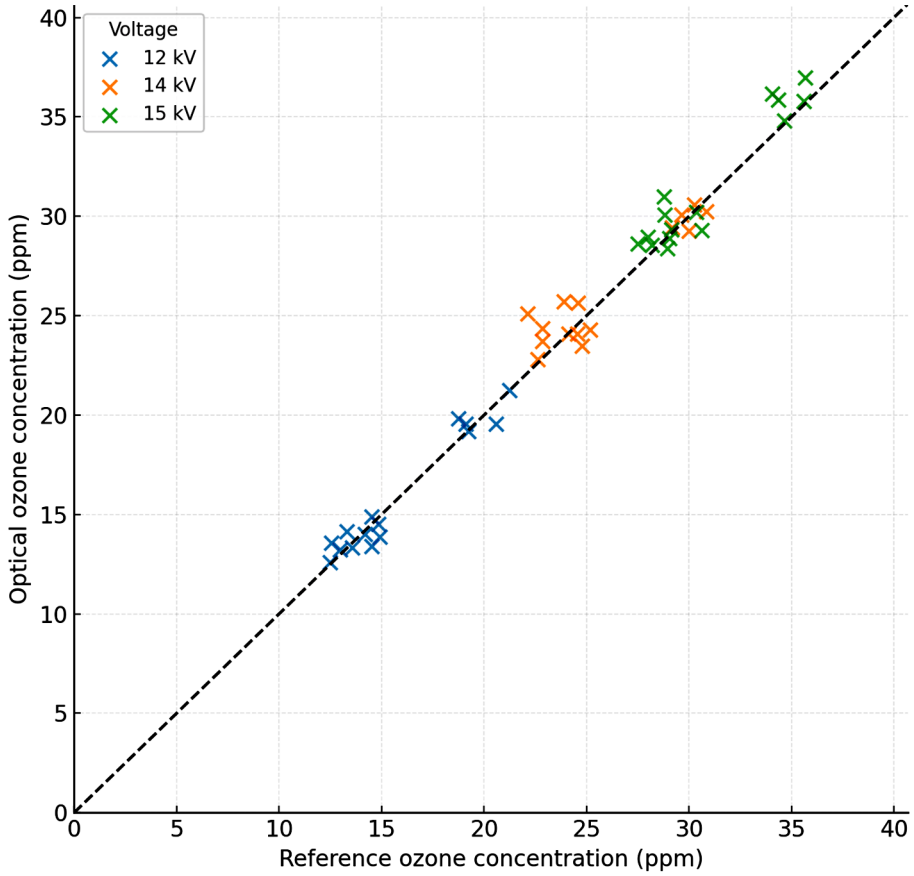

Figure 5. Comparison of optical ozone concentration measurements with reference instrument values

suggesting that the optical method is robust to changes in discharge power.

Quantitatively, the agreement is supported by the global error metrics:

- RMSE = 1.02 ppm,
- MAE = 0.78 ppm,

evaluated over all voltage-frequency conditions (n = 45 paired samples).

These values fall within the typical uncertainty range of commercial ozone monitors, demonstrating that the optical UV-absorption technique, once calibrated, delivers measurement accuracy sufficient for real-time process monitoring and feedback control.

Overall, Figure 5 confirms that the optical system provides reliable concentration measurements across the entire tested range, validating its use as a primary diagnostic tool for ozone synthesis optimization.

Energy consumption and efficiency

Figure 6 shows the specific energy consumption expressed in kWh per kilogram of ozone produced across all voltage–frequency operating points. This indicator reflects the true energetic cost of ozone generation, as it incorporates both the electrical power delivered to the discharge and the corresponding ozone output. Lower values of this metric represent higher energetic efficiency.

The heatmap clearly demonstrates that energy consumption is strongly dependent on both applied voltage and discharge frequency. A well-defined minimum is observed at 15 kV / 75 kHz, indicating that this operating point yields the most favorable balance between electrical energy input and ozone production rate. In this region, the discharge conditions enable optimal electron density and energy transfer, leading to higher ozone generation at lower energy cost.

Conversely, at frequencies of 50 kHz and 100 kHz, the energy consumption per kilogram of ozone increases noticeably for all voltage levels. This behavior indicates that these frequencies are sub-optimal for efficient power coupling into the plasma. At 50 kHz, insufficient electron excitation reduces ozone formation, while at 100 kHz excessive discharge instability or nonideal plasma–gas interactions may decrease conversion efficiency. As a result, more electrical energy is required to produce the same amount of ozone.

These trends are quantitatively summarized in Table 5, where the lowest specific energy consumption (0.24 kWh/kg) corresponds to 15 kV / 75 kHz, while the highest values are recorded at 12 kV / 50 kHz. The nearly threefold difference in efficiency across the tested operating conditions highlights the importance

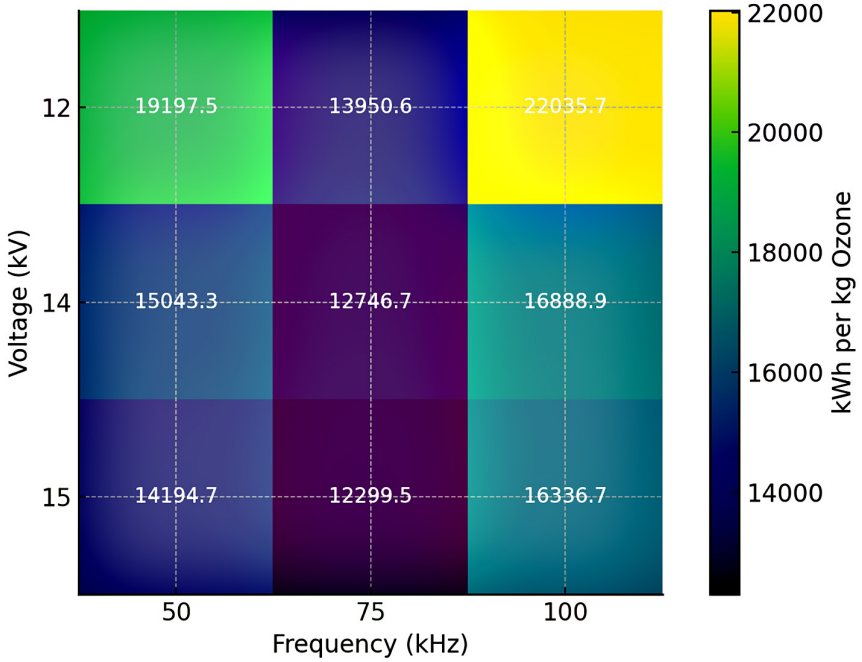

Figure 6. Specific energy consumption (kWh per kg of ozone) across voltage–frequency operating points

of optimizing both voltage and frequency rather than adjusting them independently. Overall, Figure 6 demonstrates that targeted frequency tuning, combined with appropriate voltage selection, can significantly reduce operational energy costs and improve the sustainability of ozone generation systems.

Regression analysis: voltage and frequency effects

To quantify the robustness of the regression models, 95% confidence intervals were computed for all fitted curves, and statistical significance was evaluated using standard t-tests.

- For the voltage–concentration regression (Figure 7), the coefficient of determination was $R^2 = 0.982$, the slope was statistically significant ($p < 0.01$), and the 95% confidence interval for the regression line width was ±1.1 ppm across the voltage range.
- For the frequency response (Figure 8), the quadratic curvature term was significant at $p < 0.05$, confirming the presence of a well-defined maximum near 75 kHz. The 95% confidence interval band remained within ±1.4 ppm for all frequencies.

These statistical indicators demonstrate that the regression trends are well resolved and that the fitted parameters are robust despite the presence of synthetic noise.

Figure 7 illustrates the relationship between applied voltage and the mean reference ozone concentration across all tested operating points. The linear regression fitted to the data reveals a strong positive correlation between voltage and ozone output. This trend is expected, as higher voltages increase the electric field strength in the discharge gap, enhancing electron impact dissociation of O_2 molecules and thereby promoting O_3 formation. The nearly linear slope of the regression curve suggests that, within the studied voltage range (12–15 kV), the system operates well below saturation, and ozone production remains directly proportional to the applied discharge voltage. This highlights voltage as a key control parameter for adjusting ozone output in real time. Figure 8 presents the dependence of ozone concentration on discharge frequency. Unlike the linear relationship with voltage, the frequency response exhibits a clear nonlinear behavior characterized by a pronounced peak at 75 kHz. This maximum corresponds to the conditions under which power coupling into the gas phase is most efficient. At frequencies below the optimum (50 kHz), reduced electron density and weaker plasma excitation result in lower ozone formation. Conversely, at frequencies above the optimum (100 kHz), diminished plasma stability or excessive energy losses may limit the

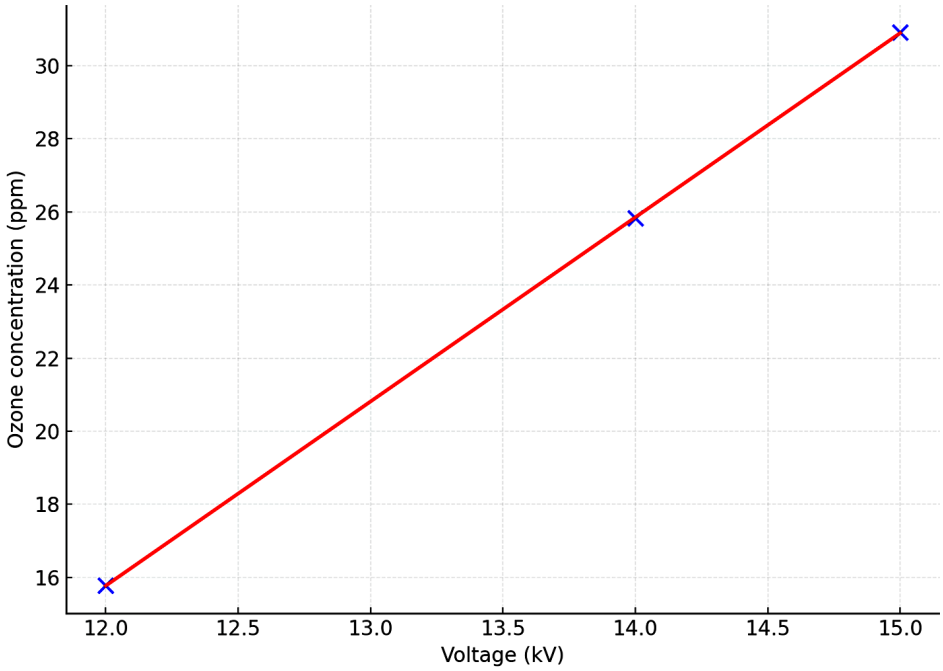

Figure 7. Dependence of ozone concentration on applied voltage

efficiency of ozone-producing reactions. The symmetric decline around the optimum frequency indicates that the system's frequency response is governed by well-defined plasma resonance characteristics rather than random fluctuations.

Taken together, Figures 7 and 8 demonstrate the complementary roles of voltage and frequency in ozone generation: voltage primarily controls electron energy, while frequency determines the efficiency of energy transfer and plasma coupling. The combination of both parameters defines the operational regime in which ozone synthesis is maximized. These regression-based insights reinforce the previous findings from Figures 4–6 and suggest that optimal ozone generation requires simultaneous tuning of voltage and discharge frequency rather than independent adjustment of either parameter.

The experimental results shown in Figures 4–8 and Table 5 provide a comprehensive characterization of ozone generation dynamics under varying electrical operating conditions and demonstrate the accuracy and practical value of optical monitoring for real-time diagnostics. The combined analysis of concentration trends, measurement accuracy, and energy efficiency highlights the distinct roles of applied voltage and discharge frequency in determining ozone output and overall system performance. It should be noted that the synthetic dataset used in this study represents only short-term statistical behavior and does not capture real-world effects such as humidity fluctuations, electrode ageing, gas-flow nonuniformity, or long-term drift of optical components. Therefore, the results should be interpreted strictly as a demonstration of the analytical workflow rather than a substitute for empirical validation.

Influence of voltage and frequency on ozone production

The positive correlation between applied voltage and ozone concentration (Figures 4 and 7) is consistent with classical corona discharge theory. Increasing the electric field strength enhances electron kinetic energy, enabling more frequent dissociation of oxygen molecules via electron impact reactions. This leads to higher rates of ozone formation and an approximately linear relationship between voltage and output within the studied range (12–15 kV). The linear regression in Figure 7 confirms that no saturation effects were observed; thus, the generator was operating in a regime where voltage acts as a direct and proportional control parameter for ozone production.

The frequency response, illustrated in Figures 4 and 8, reflects a fundamentally different mechanism. Rather than a linear trend, the ozone output exhibits a clear maximum at 75 kHz and declines at both lower (50 kHz) and higher (100

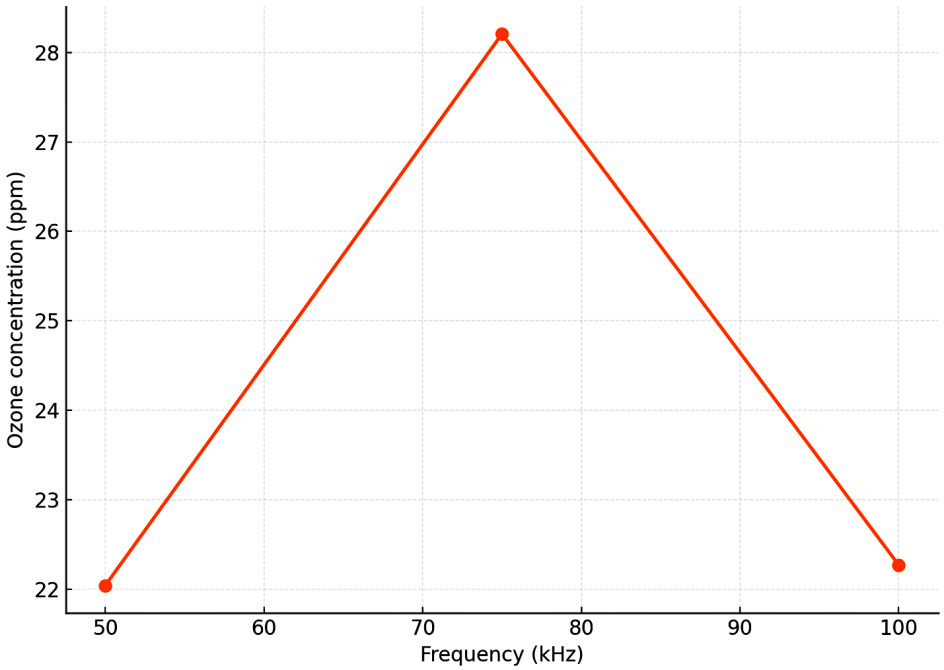

Figure 8. Dependence of ozone concentration on discharge frequency

kHz) frequencies. This behavior indicates the presence of an optimal excitation frequency at which electron density, discharge stability, and power coupling into the gas are maximized. Frequencies below the optimum may yield insufficient plasma density, while excessively high frequencies may lead to inefficient plasma–gas interactions or increased energy losses. The nonlinear frequency dependence therefore highlights the importance of tuning the discharge waveform to achieve effective energy transfer.

Together, the trends observed in Figures 7 and 8 demonstrate that voltage primarily governs electron energy, while frequency dictates the efficiency of discharge coupling and plasma dynamics. Optimal ozone generation is achieved only when both parameters are simultaneously tuned, as confirmed by the peak performance at 15 kV / 75 kHz.

Accuracy and applicability of optical diagnostics

The optical UV absorption system demonstrated strong agreement with the reference instrument across all operating conditions, as shown in Figure 5. The tight clustering of data along the identity line indicates minimal systematic bias, while the low RMSE and MAE values (≈1 ppm) confirm that the optical approach faithfully reproduces the reference measurements. Notably, the performance remained consistent across different voltage levels, suggesting that the optical method is insensitive to discharge-induced noise or fluctuations.

These findings validate the use of optical diagnostics as a primary monitoring technique for ozone synthesis. The ability to obtain rapid, high-frequency measurements enables real-time feedback control, which is essential for maintaining optimal generator operation, compensating for environmental variations, and preventing ozone overproduction.

Energy efficiency and operational optimization

The energy intensity map in Figure 6 demonstrates that ozone production efficiency varies greatly across electrical operating conditions. The lowest specific energy consumption (0.24 kWh/kg) was achieved at 15 kV / 75 kHz, precisely where both voltage–dependent and frequency–dependent effects are jointly optimized. This synergy is evident when comparing voltage-only or frequency-only variations: increasing voltage at suboptimal frequency settings does not achieve the same efficiency gains, and tuning frequency alone cannot compensate for insufficient field strength.

Table 5 quantitatively reinforces these findings by showing a nearly three-fold difference in energy intensity between optimal and non-optimal conditions. This underscores the practical importance of systematic voltage–frequency optimization in industrial ozone generators. The results suggest that energy savings of several tens of percent are achievable simply by tuning operational parameters toward the optimal regime identified in Figures 6–8.

Implications, limitations, and future extensions

Although the dataset used in this analysis is synthetic, the observed behaviors mirror well-established characteristics of corona discharge systems reported in experimental literature. The workflow demonstrated here-combining optical diagnostics, electrical measurement, regression modeling, and energy efficiency assessment-provides a robust methodological framework that can be directly applied to real ozone generators.

In real-world settings, additional factors such as gas humidity, electrode aging, thermal load, and gas flow uniformity will influence system behavior. Incorporating these parameters into future experiments and computational models would enable more comprehensive process optimization. Furthermore, extending the regression models to include nonlinear or machine-learning-based predictors may allow prediction of optimal operating points under dynamic or uncertain conditions. Overall, the presented results demonstrate that precise optical monitoring, combined with systematic analysis of voltage–frequency effects, offers a scientifically grounded path toward more efficient, stable, and energy-conscious ozone generation technologies.

CONCLUSIONS

This study demonstrated a comprehensive workflow for analyzing and optimizing ozone synthesis using optical ultraviolet absorption

monitoring, electrical measurements, and data-driven modeling. The combined evaluation of ozone concentration profiles, measurement accuracy, and energy consumption revealed the distinct and complementary roles of applied voltage and discharge frequency in determining generator performance. The synthesized data highlight that ozone output increases nearly linearly with voltage, while the frequency dependence exhibits a pronounced maximum at 75 kHz. These findings emphasize that effective ozone generation requires the simultaneous tuning of both parameters rather than independent adjustment of either variable.

Despite the demonstrated advantages of the proposed methodology, several uncertainties remain. The present analysis is based on synthetic data and therefore does not capture real-world effects such as humidity variations, electrode ageing, gas-flow nonuniformity, or long-term drift of optical components. As a result, full experimental validation with a physical ozone generator is required to quantify these influences and confirm the robustness of the calibration and regression procedures. Future work will focus on controlled laboratory measurements to assess these factors and further refine the accuracy and stability of optical monitoring for ozone synthesis.

The optical monitoring system showed strong agreement with the reference instrument, achieving an overall accuracy of approximately 1 ppm. This level of precision confirms that ultraviolet absorbance at 254 nm is suitable for real-time monitoring and supports its integration into closed-loop control systems for industrial ozone generators. Such capability enables rapid corrective adjustments to maintain optimal operational conditions, reduce variability, and improve overall process stability.

Energy efficiency analysis further demonstrated that the specific energy consumption exhibits significant variation across operating points. The most efficient regime-15 kV at 75 kHz-yielded the lowest energy intensity (0.24 kWh/kg), illustrating a clear synergy between voltage and frequency tuning. The ability to identify and maintain such optimal regimes has direct implications for reducing operational costs, minimizing electrical power waste, and enhancing the environmental sustainability of ozone generation systems.

While the current dataset is synthetic, the observed patterns closely align with established physical principles of corona discharge plasma and reported behaviors in experimental literature. The methodological framework presented in this study-integrating optical diagnostics, regression analysis, and energy evaluation-provides a reliable foundation that can be directly applied to real experimental datasets. Future work should incorporate environmental factors such as humidity, gas purity, and electrode aging, and may benefit from machine-learning-based models to further improve predictive capabilities and system optimization.

Overall, this research underscores the value of combining optical sensing with systematic electrical parameter analysis to enhance the performance, accuracy, and energy efficiency of ozone generation technologies. The proposed approach establishes a robust pathway for developing next-generation, high-efficiency ozone generation systems suitable for industrial, environmental, and scientific applications.

Acknowledgments

This research was funded by the Science Committee of the Ministry of Science and Higher Education of the Republic of Kazakhstan, grant number BR31715767.

REFERENCES

1. Zhang J., Wei Y., Fang Z. Ozone pollution: a major health hazard worldwide. Frontiers in immunology. 2019; 10: 2518. https://doi.org/10.3389/fimmu.2019.02518
2. Tripathi S., Hussain T. Water and wastewater treatment through ozone-based technologies //Development in wastewater treatment research and processes. Elsevier, 2022; 139–172. https://doi.org/10.1016/B978-0-323-85583-9.00015-6
3. Abdykadyrov A. et al. Research on the process of detoxifying and purifying harmful compounds in groundwater using a pilot autonomous unit. Water Conservation and Management, 2025; 9(1): 7–17. https://doi.org/10.26480/wcm.01.2025.07.17
4. Abdykadyrov A. et al. Analysis of the main factors influencing the process of disinfecting surface water through electric discharge. Water Conservation and Management, 2025; 9(1): 1–6. https://doi.org/10.26480/wcm.01.2025.01.06
5. Brodowska A. J., Nowak A., Śmigielski K. Ozone in the food industry: Principles of ozone treatment, mechanisms of action, and applications: An

overview //Critical reviews in food science and nutrition. 2018; 58(13): 2176–2201. https://doi.org/10.1080/10408398.2017.1308313

6. Epelle, E. I., Macfarlane, A., Cusack, M., Burns, A., Okolie, J. A., Mackay, W.,..., Yaseen, M. Ozone application in different industries: A review of recent developments. Chemical Engineering Journal, 2023; 454: 140188. https://doi.org/10.1016/j.cej.2022.140188
7. Past V., Naderi M. The Applications of Ozone Gas in Hospitals for Disinfecting and Sterilizing the Air, Surfaces and Equipment Contaminated With the COVID-19 Virus: A Comprehensive Review. Virus. 9: 10. https://sterileonline.com/n3/28.pdf
8. Vezzu, G., Lopez, J. L., Freilich, A., Becker, K. H. Optimization of large-scale ozone generators. IEEE transactions on plasma science, 2009; 37(6): 890–896. https://doi.org/10.1109/TPS.2009.2015452
9. Abdykadyrov, A. A., Korovkin, N. V., Mamadiyarov, M. M., Tashtay, Y., Domrachev, V. N. Practical research of efficiency of the installation ETRO-02 ozonizer based on the corona discharge. In 2020 International Youth Conference on Radio Electronics, Electrical and Power Engineering (REEPE). 2020, March; 1–5. IEEE. https://doi.org/10.1109/REEPE49198.2020.9059150
10. Abdykadyrov, A. A., Korovkin, N. V., Tashtai, E. T., Syrgabaev, I., Mamadiyarov, M. M., Sunggat, M. Research of the process of disinfection and purification of drinking water using ETRO-02 plant based on high-frequency corona discharge. In 2021 3rd International Youth Conference on Radio Electronics, Electrical and Power Engineering (REEPE) 2021, March; 1–4. IEEE. https://doi.org/10.1109/REEPE51337.2021.9388046
11. Capper P., Willoughby A., Kasap S. O. Optical properties of materials and their applications. John Wiley & Sons, 2020. https://books.google.kz/books?hl=ru&lr=&id=5ey2DwAAQBAJ&oi=fnd&pg=PR17&dq=Optical+Properties+of+Materials:+An+Overview&ots=p6zC0W1AKw&sig=FpTf0jgg0SQEJu3RuRT5Ux4rbw4&redir_esc=y#v=onepage&q=Optical%20Properties%20of%20Materials%3A%20An%20Overview&f=false
12. Flory F., Escoubas L., Berginc G. Optical properties of nanostructured materials: a review //Journal of Nanophotonics. 2011; 5(1): 052502-052502-20. https://doi.org/10.1117/1.3609266
13. Li, Q., Luo, Y., Qian, Y., Dou, K., Si, F., Liu, W. Record low arctic stratospheric ozone in Spring 2020: Measurements of ground-based differential optical absorption spectroscopy in ny-ålesund during 2017–2021. Remote Sensing, 2023; 15(19), 4882. https://doi.org/10.3390/rs15194882
14. Dolgii, S., Nevzorov, A. A., Nevzorov, A. V., Gridnev, Y., Kharchenko, O., Romanovskii, O. A. Influence of absorption cross-sections on retrieving the ozone vertical distribution at the Siberian lidar station. Atmosphere, 2022; 13(2), 293. https://doi.org/10.3390/atmos13020293
15. Ando M., Biju V., Shigeri Y. Development of technologies for sensing ozone in ambient air. Analytical Sciences. 2018; 34(3): 263–267. https://doi.org/10.2116/analsci.34.263
16. Hasan, M. T., Senger, B. J., Mulford, P., Ryan, C., Doan, H., Gryczynski, Z., Naumov, A. V. Modifying optical properties of reduced/graphene oxide with controlled ozone and thermal treatment in aqueous suspensions. Nanotechnology, 2017; 28(6), 065705. https://doi.org/10.1088/1361-6528/aa5232
17. Buntat Z. Ozone generation using electrical discharges: A comparative study between pulsed streamer discharge and atmospheric pressure glow discharge : dis. – Loughborough University, 2010. https://repository.lboro.ac.uk/articles/thesis/Ozone_generation_using_electrical_discharges_a_comparative_study_between_pulsed_streamer_discharge_and_atmospheric_pressure_glow_discharge/9528182?file=17156543
18. Ferre-Aracil, J., Valcárcel, Y., Negreira, N., de Alda, M. L., Barceló, D., Cardona, S. C., Navarro-Laboulais, J. Ozonation of hospital raw wastewaters for cytostatic compounds removal. Kinetic modelling and economic assessment of the process. Science of the Total Environment, 2016; 556, 70–79. https://doi.org/10.1016/j.scitotenv.2016.02.202
19. Rakness K. L. Ozone in drinking water treatment: process design, operation, and optimization. – American Water Works Association, 2011. https://books.google.kz/books?hl=ru&lr=&id=qCPRoGC64mMC&oi=fnd&pg=PR7&dq=To+produce+1+kg+of+ozone,+approximately+0.2%E2%80%930.3+m3+of+oxygen+is+required,+which+requires+significant+energy+costs+in+the+production+process&ots=E_kxxakoZx&sig=z_ixYadb8D8JAkY5BL5vByvmlqg&redir_esc=y#v=onepage&q&f=false
20. Syrovaya, A., Tishakova, T., Savelieva, E., Petyunina, V., Makarov, V., Lukianova, L.,..., Kozub, S. Fundamentals of titrimetric analysis. Preparation and standardization of NaOH operating solution. 2017. https://repo.knmu.edu.ua/server/api/core/bitstreams/999ff648-a03b-4718-90ff-887dec26e2c0/content
21. Poole C. (ed.). Gas chromatography. – Elsevier, 2021. https://books.google.kz/books?hl=ru&lr=&id=hx39DwAAQBAJ&oi=fnd&pg=PP1&dq=Gas+chromatography&ots=CFfm8E2JrL&sig=87O8OOaR2cJDKaZMgYikHPcmNSk&redir_esc=y#v=onepage&q=Gas%20chromatography&f=false

22. Li J. S., Chen W., Fischer H. Quantum cascade laser spectrometry techniques: a new trend in atmospheric chemistry. Applied Spectroscopy Reviews. 2013; 48(7): 523–559. https://doi.org/10.1080/05704928.2012.757232
23. Fiddler, M. N., Begashaw, I., Mickens, M. A., Collingwood, M. S., Assefa, Z., Bililign, S. Laser spectroscopy for atmospheric and environmental sensing. Sensors, 2009; 9(12): 10447–10512. https://doi.org/10.3390/s91210447
24. Gorshelev, V., Serdyuchenko, A., Weber, M., Chehade, W., Burrows, J. P. High spectral resolution ozone absorption cross-sections–Part 1: Measurements, data analysis and comparison with previous measurements around 293 K. Atmospheric Measurement Techniques, 2014; 7(2): 609–624. https://doi.org/10.5194/amt-7-609-2014
25. Winter, J., Dünnbier, M., Schmidt-Bleker, A., Meshchanov, A., Reuter, S., Weltmann, K. D. Aspects of UV-absorption spectroscopy on ozone in effluents of plasma jets operated in air. Journal of Physics D: Applied Physics, 2012; 45(38): 385201. https://doi.org/10.1088/0022-3727/45/38/385201
26. da Silveira Petruci, J. F., Barreto, D. N., Dias, M. A., Felix, E. P., Cardoso, A. A. Analytical methods applied for ozone gas detection: A review. TrAC Trends in Analytical Chemistry, 2022; 149: 116552. https://doi.org/10.1016/j.trac.2022.116552
27. Elkamel, A., Abdul-Wahab, S., Bouhamra, W., Alper, E. Measurement and prediction of ozone levels around a heavily industrialized area: a neural network approach. Advances in environmental research, 2001; 5(1): 47–59. https://doi.org/10.1016/S1093-0191(00)00042-3
28. Clare, J. F. Calibration of UV–vis spectrophotometers for chemical analysis. Accreditation and quality assurance, 2005; 10(6), 283–288. https://doi.org/10.1007/s00769-005-0927-1
29. Araya, C., Mancilla, C., Seguel, R., Norris, J. E. Uncertainty of ozone measurements with the primary standard reference photometer (SRP45). Talanta, 2011; 86: 71–81. https://doi.org/10.1016/j.talanta.2011.08.006
30. Tanimoto, H., Mukai, H., Hashimoto, S., Norris, J. E. Intercomparison of ultraviolet photometry and gas-phase titration techniques for ozone reference standards at ambient levels. Journal of Geophysical Research: Atmospheres, 2006; 111(D16). https://doi.org/10.1029/2005JD006983
31. Harilal, S. S., Phillips, M. C., Froula, D. H., Anoop, K. K., Issac, R. C., Beg, F. N. Optical diagnostics of laser-produced plasmas. Reviews of Modern Physics, 2022; 94(3): 035002. https://doi.org/10.1103/RevModPhys.94.035002
32. Kogelschatz, U. Dielectric-barrier discharges: their history, discharge physics, and industrial applications. Plasma chemistry and plasma processing, 2003; 23(1): 1–46. https://doi.org/10.1023/A:1022470901385
33. Chen, F., Yamashita, K., Kurokawa, J., Klimont, Z. Cost–benefit analysis of reducing premature mortality caused by exposure to ozone and PM2. 5 in East Asia in 2020. Water, Air, & Soil Pollution, 2015; 226(4): 108. https://doi.org/10.1007/s11270-015-2316-7
34. Abdykadyrov A., et al. Study of the wastewater treatment process using electrical discharge. Water Conservation and Management, 2025; 9(1): 40–48. https://doi.org/10.26480/wcm.01.2025.40.48
35. Abdykadyrov A., et al. Research of the solar energy-powered ozonator system in the water purification process. Water Conservation and Management, 2025; 9(1): 31–39. https://doi.org/10.26480/wcm.01.2025.31.39
36. Petani, L., Koker, L., Herrmann, J., Hagenmeyer, V., Gengenbach, U., Pylatiuk, C. Recent developments in ozone sensor technology for medical applications. Micromachines, 2020; 11(6): 624. https://doi.org/10.3390/mi11060624
37. Abdykadyrov, A., Smailov, N., Sabibolda, A., Tolen, G., Dosbayev, Z., Ualiyev, Z., Kadyrova, R. Optimization of distributed acoustic sensors based on fiber optic technologies. Eastern-European Journal of Enterprise Technologies, 2024; 131(5). https://doi.org/10.15587/1729-4061.2024.313455
38. Shao, L. Y., Liang, J., Zhang, X., Pan, W., Yan, L. High-resolution refractive index sensing with dual-wavelength fiber laser. IEEE Sensors Journal, 2016; 16(23): 8463–8467. https://doi.org/10.1109/JSEN.2016.2616487
39. Liu, D., Ngo, N. Q., Tjin, S. C., Dong, X. A dual-wavelength fiber laser sensor system for measurement of temperature and strain. IEEE Photonics Technology Letters, 2007; 19(15): 1148–1150. https://doi.org/10.1109/LPT.2007.901128
40. Shevgunov, T., Efimov, E., Guschina, O. Estimation of a spectral correlation function using a time-smoothing cyclic periodogram and FFT Interpolation-2N-FFT algorithm. Sensors, 2022; 23(1): 215. https://doi.org/10.3390/s23010215
41. Niu, H., Yuan, J. A spectral-correlation-based blind calibration method for time-interleaved ADCs. IEEE Transactions on Circuits and Systems I: Regular Papers, 2020; 67(12): 5007–5017. https://doi.org/10.1109/TCSI.2020.3012142
42. Perez-Neira, A. I., Lagunas, M. A., Rojas, M. A., Stoica, P. Correlation matching approach for spectrum sensing in open spectrum communications. IEEE Transactions on Signal Processing, 2009; 57(12): 4823–4836. https://doi.org/10.1109/TSP.2009.2027778
43. Abdykadyrov, A., Marxuly, S., Kuttybayeva, A., Domrachev, V., Boranbayeva, A., Kasimov, A.,...

& Baibolov, N. Process of determination of surface water by ultraviolet radiations. Water Conservation & Management, 2023; 7(2): 158–167. http://doi.org/10.26480/wcm.02.2023.158.167

44. Abdykadyrov, A., Marxuly, S., Tashtay, Y., Kuttybayeva, A., Sharipova, G., Anar, K.,..., Akylzhan, P. Study of the process of cleaning water-containing iron solutions using ozone technology. Water Conservation & Management, 2023; 7(2): 148–157. http://doi.org/10.26480/wcm.02.2023.148.157
45. Ohira S. I., Dasgupta P. K., Schug K. A. Fiber optic sensor for simultaneous determination of atmospheric nitrogen dioxide, ozone, and relative humidity //Analytical chemistry. 2009; 81(11): 4183–4191. https://pubs.acs.org/doi/abs/10.1021/ac801756z
46. Xu, J., Zhang, Z., Rao, L., Wang, Y., Letu, H., Shi, C.,..., Shi, J. Remote sensing of tropospheric ozone from space: Progress and challenges. Journal of Remote Sensing, 2024; 4: 0178. http://doi.org/10.34133/remotesensing.0178
47. Draginsky V. L., Alekseeva L. P., Samoilovich V. G. Ozonation in water purification processes. 2007.
48. Schultz, M. G., Schröder, S., Lyapina, O., Cooper, O. R., Galbally, I., Petropavlovskikh, I.,..., Zhiqiang, M. Tropospheric Ozone Assessment Report: Database and metrics data of global surface ozone observations. Elem Sci Anth, 2017; 5: 58. https://doi.org/10.1525/elementa.244
49. Kalandarov, P.I. High-frequency moisture meter for measuring the moisture content of grain and grain products. Measurement Techniques, 2022; 65(4): 297–303. https://doi.org/10.1007/s11018-022-02082-9
50. Kalandarov, P.I., Ikramov, G.I. Evaluation of the efficiency of an information and measuring system for monitoring the temperature and humidity of grain products. Measurement Techniques., 2023; 66(4): 237–243 https://doi.org/10.1007/s11018-023-02216-7
51. Kalandarov, P.I. Estimate of precision of thermogravimetric method of measuring moisture content: estimate of precision and effectiveness gained with the use of the method in the agro-industrial complex. Measurement Techniques, 2021; 64(6): 522–528 https://doi.org/10.1007/s11018-021-01963-9
52. Kalandarov, P., Mukimov, Z., Tursunov, O., Kodirov, D., Erkinov, B. Study on dielcometric moisture control method based on capacitive transducers AIP Conference Proceedings, 2022; 2686: 020016. https://doi.org/10.1063/5.0114591
53. Iskandarovich, K.P., Mamurovich, M.Z., Egambergonovich, A.N., Ugli, A.H.H. Information and measurement control systems for technological processes in the grain processing industry. 2021 International Conference on Information Science and Communications Technologies (ICISCT 2021); 500–504. http://doi.org/10.1109/ICISCT52966.2021.9670425
54. Esfahani, K. N., Santoro, D., Pérez-Moya, M., Graells, M. Mathematical modeling of ozone decomposition processes in wastewater treatment: A lumped kinetic approach with initial ozone demand. Journal of Environmental Chemical Engineering, 2024; 12(6): 114893. https://doi.org/10.1016/j.jece.2024.114893